Mercury−Chalcogenide Clusters: Synthesis and Structure of $[Hg_{10}Te_4(SePh)_{12}(PPhnPr_2)_4]$, $[Hg_{10}Te_4(TePh)_{12}(PPhnPr_2)_4]$ and $[Hg_{34}Te_{16}(SePh)_{36}(PPhnPr_2)_4]$

Andreas Eichhöfer*[a] and Peter Deglmann[b]

Keywords: Cluster compounds / Mercury / Tellurium / Selenium / DFT calculations

The reaction of $HgCl_2$ with $PPhnPr_2$, $Te(SinBu_3)_2$ and $PhESiMe_3$ (E = Se, Te) in DME at –30 °C results in the formation of yellow octahedral crystals of $[Hg_{10}Te_4(SePh)_{12}(PPhnPr_2)_4]$ and $[Hg_{10}Te_4(TePh)_{12}(PPhnPr_2)_4]$ respectively. The molecular structures of the clusters are similar to those of other $[M_{10}Se_4(SePh)_{12}(PR_3)_4]$ (M = Cd, Zn; R = org. group) cluster compounds, but are the first of this type with tellurium as the group 16 metal atom. Dissolution of $[Hg_{10}Te_4(SePh)_{12}(PPhnPr_2)_4]$ in benzene/toluene at 5 °C leads to the formation of the larger cluster $[Hg_{34}Te_{16}(SePh)_{36}(PPhnPr_2)_4]$ which displays a new structure type for group 12–16 cluster molecules. The "$Hg_{34}Te_{16}Se_{36}$" cluster core can be considered as an idealized tetrahedral fragment, 15 Å in diameter, of the cubic sphalerite lattice with a vacancy in the center. Theoretical investigations on the basis of density functional theory (DFT) reproduce the structural data and the measured electronic spectra for this cluster. Additionally we found that formal occupation of the vacancy by a mercury ion would lead to an ionic cluster $[Hg_{35}Te_{16}(SeMe)_{36}(PMe_3)_4]^{2+}$ which should be stable according to the results of the calculations. This suggests that the formation of the vacancy is probably driven by the absence of an appropriate counterion in the reaction which might stabilize such an ionic cluster molecule.

Introduction

Systematic studies of the size dependent optical and electronic properties of CdSe cluster-molecules show that the quantum confinement effect common with larger CdSe nanocrystals also occurs in these small molecular systems.[1] Synthesis and structural characterization of group 12−16 cluster molecules has mostly focused on ZnS,[2] ZnSe,[3] ZnTe[4] and CdS.[5,6] Chalcogenide cluster compounds with mercury are still rare even though these materials possess interesting properties as bulk- or nano-materials. The alloy $Cd_{1-x}Hg_xTe$ is a well known material in long-wavelength IR detector technologies for example, and HgTe nanoparticles have been proposed as potential amplifiers operating at wavelengths of 1.3 μm and 1.55 μm in telecommunication devices.[7,8] Recent investigations on mercury selenide clusters reveal that the smaller cluster $[Hg_{10}Se_4(SePh)_{12}(PPh_2nPr)_4]$ is converted in benzene to a larger cluster $[Hg_{32}Se_{14}(SePh)_{36}]$.[9,10] In order to extend optical investigations on group 12−16 cluster molecules and to study further the mechanism of structural growth of nanoclusters in this size regime we investigated the synthesis and crystallization of mercury selenide and mercury telluride cluster molecules.

[a] Institut für Nanotechnologie (INT), Forschungszentrum Karlsruhe
Postfach 3640, 76021 Karlsruhe, Germany
Fax: (internat.) + 49-7247-82-6368
E-mail: eichhoefer@int.fzk.de
[b] Institut für Physikalische Chemie, Lehrstuhl für Theoretische Chemie Universität Karlsruhe,
Kaiserstr. 12, 76128 Karlsruhe, Germany

Results and Discussion

Synthesis and Structure

The reaction of $HgCl_2$ with $PPhnPr_2$, $Te(SinBu_3)_2$ and $PhESiMe_3$ (E = Se, Te) in DME at −30 °C results in the formation of yellow octahedral crystals of $[Hg_{10}Te_4(SePh)_{12}(PPhnPr_2)_4]$ (**1**) and $[Hg_{10}Te_4(TePh)_{12}(PPhnPr_2)_4]$ (**2**), respectively (Scheme 1).

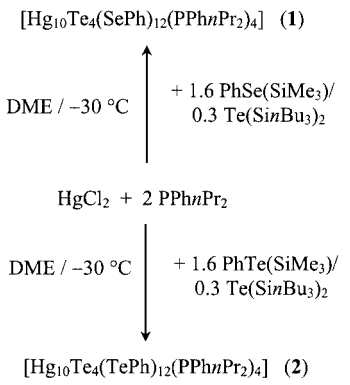

Scheme 1

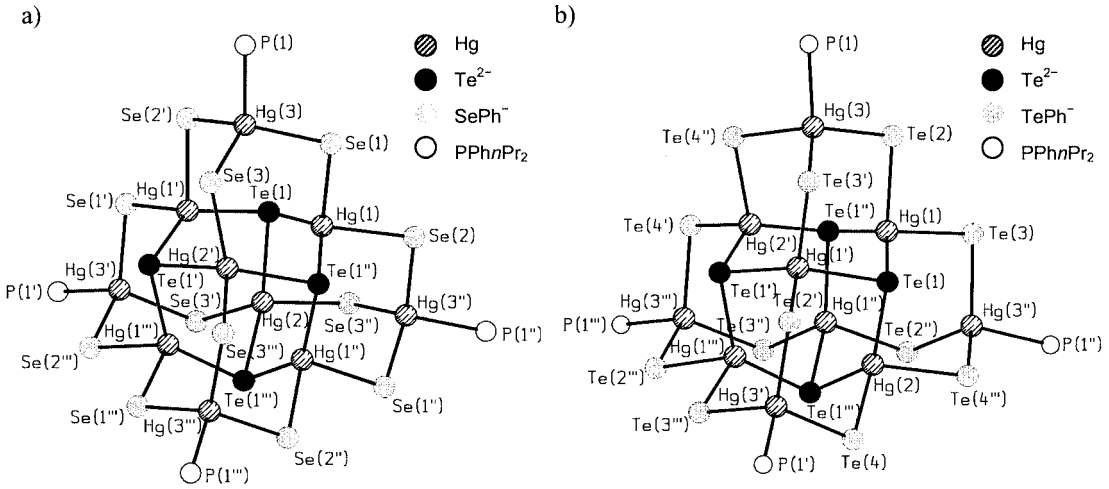

Figure 1. a) The $Hg_{10}Te_4Se_{12}P_4$ cluster core as a section of the molecular structure of $[Hg_{10}Te_4(SePh)_{12}(PPhnPr_2)_4]$ (**1**) (symmetry transformations for generating equivalent atoms: $-y + 1/4$, $x + 1/4$, $-z + 1/4$; $y - 1/4$, $-x + 1/4$, $-z + 1/4$; $-x$, $-y + 1/2$, z; $-x$, $-y + 1$, $-z + 1$). b) The $Hg_{10}Te_{16}P_4$ cluster core as a section of the molecular structure of $[Hg_{10}Te_4(TePh)_{12}(PPhnPr_2)_4]$ (**2**) (symmetry transformations for generating equivalent atoms: $y - 1/4$, $-x + 1/4$, $-z + 1/4$; $-y + 1/4$, $x + 1/4$, $-z + 1/4$; $-x$, $-y + 1/2$, z). C and H atoms are omitted for clarity.

Figure 1(a) shows the molecular structure of the $[Hg_{10}Te_4Se_{12}P_4]$ cluster core of **1** determined by single-crystal X-ray diffraction (see also Table 3). The compound crystallizes in the tetragonal space group $I4_1/a$ (4bar site symmetry). The cluster core, which is comprised of four adamantane cages each of which is formed by three tellurium, three selenium and four mercury atoms, is a macrotetrahedral fragment of the sphalerite structure, which is also found in HgSe and HgTe.[11] The resultant tetrahedron, with the four phosphane atoms in the apex positions, has edge lengths of 1240.6−1284.2 pm and has a diameter of 820 pm (from the mercury atom at the vertex of the tetrahedron to the center of the opposite tetrahedral face).

The mercury atoms Hg1−Hg3 have distorted tetrahedral environments, coordinated by the selenium atoms of the μ_2-$SePh^-$ ligands (Se1, Se2, Se3) and the μ_3-Te^{2-} ligands (Te1) as well as the phosphorus atoms of the $PPhnPr_2$ ligands (P1) (bond angles are: Se−Hg−Se 96.59−112.26(3); Se−Hg−Te 92.17−113.73(3); Te−Hg−Te 134.47−137.15(4); P−Hg−Se 104.76−108.22(11)°]. The Hg−SePh bond lengths which range from 263.44−278.09(10) pm are similar to those found in $[Hg_{10}Se_4(SePh)_{12}(PPh_2nPr)_4]$[10] while the Hg−Te bond lengths between 270.92−274.13(7) pm are shorter than those in HgTe (279 pm).[12] The Hg−P1 bond length of the four outer Hg3 atoms coordinated by the $PPhnPr_2$ ligands is 256.9(3) pm.

Figure 1(b) shows the molecular structure of the $[Hg_{10}Te_{16}P_4]$ cluster core of **2** determined by single-crystal X-ray diffraction which is isostructural with **1**. Due to the larger covalent radii of the tellurium atoms the cluster core is slightly larger in comparison with **1** as indicated by edge lengths of 1289.3−1298.7 pm of the tetrahedron formed by the four phosphane atoms and a diameter of 840 pm taken from the mercury atom at the vertex of the tetrahedron to the center of the opposite tetrahedral face. The Hg−TePh bond lengths range from 278.02−291.11(11) pm corresponding to values found in $[Hg_6(\mu\text{-}Br_2)Br_2(\mu\text{-}TePh)_8(py)_2]$[13] and the Hg−Te bond lengths from

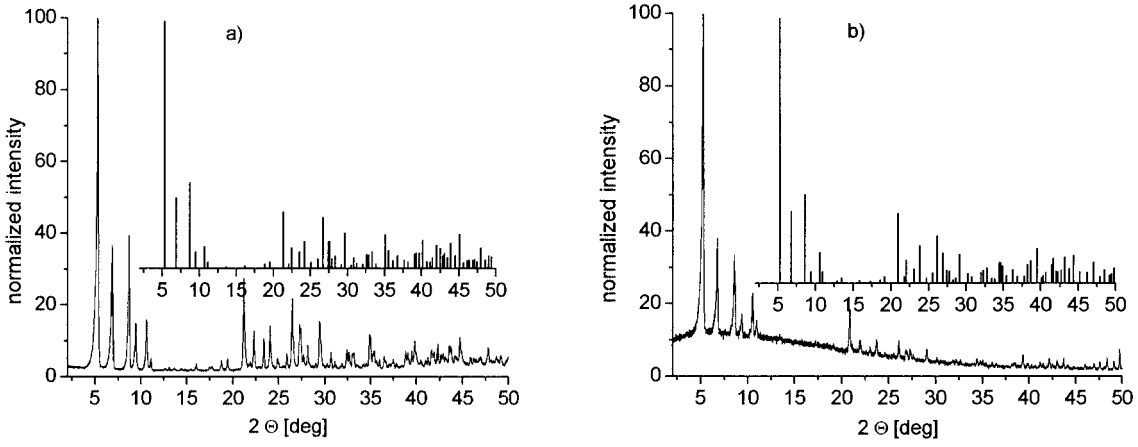

Figure 2. Measured X-ray powder pattern and calculated peak pattern for a) $[Hg_{10}Te_4(SePh)_{12}(PPhnPr_2)_4]$ (**1**) and b) $[Hg_{10}Te_4(TePh)_{12}(PPhnPr_2)_4]$ (**2**).

272.39−275.74(10) pm are similar to those in **1**. The value of the Hg−P1 bond length for the four outer Hg3 atoms coordinated by the PPh*n*Pr$_2$ ligands is 261.1(4) pm.

Filtration of **1** and **2** at −30 °C and subsequent drying in vacuo resulted in yellow powders which are stable under nitrogen at room temperature. Powder diffraction patterns of the two compounds show their crystalline purity (Figure 2). If **2** is dissolved in benzene/toluene at 5 °C the formation of an orange solution can be observed from which **3** crystallizes within a few days (Scheme 2).

$$4\ [Hg_{10}Te_4(SePh)_{12}(PPh\mathit{n}Pr_2)_4]\ \ (\mathbf{1})$$

$$\xrightarrow[5\ ^\circ C]{C_6H_6/\text{toluene}}$$

$$[Hg_{34}Te_{16}(SePh)_{36}(PPh\mathit{n}Pr_2)_4]\ \ (\mathbf{3})$$
$$+$$
$$6\ Hg(SePh)_2\ +\ 12\ PPh\mathit{n}Pr_2$$

Scheme 2

The compound crystallizes in the triclinic space group $P\bar{1}$ (see also Table 3). The $Hg_{34}Te_{16}Se_{36}$ cluster framework is formed from four fused $Hg_{10}Te_4Se_{12}$ cluster cores and thus 16 $Hg_6Te_3Se_3$ adamantane like cages with a tetrahedral hole in the center of the molecule (Figure 3).

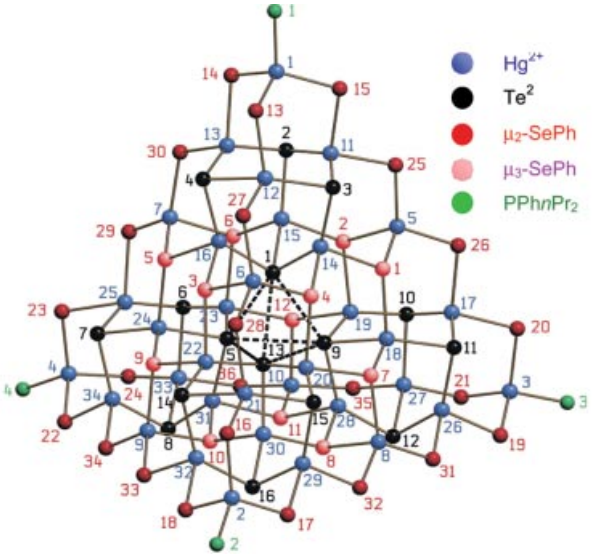

Figure 3. The $Hg_{34}Te_{16}Se_{36}P_4$ cluster core as a section of the molecular structure of $[Hg_{34}Te_{16}(SePh)_{36}(PPh\mathit{n}Pr_2)_4]$ (**3**). Atoms are labeled with numbers only. Nonbonding Te−Te distances (dashed line): Te1−Te9: 376.4 ; Te5−Te13: 385.5 pm. C and H atoms are omitted for clarity.

Thus one could formally explain the formation of **3** in terms of a direct condensation reaction of four "$Hg_{10}Te_4(SePh)_{12}$" cluster cores accompanied by the formal cleavage of six "$(PPhnPr_2)_2Hg(SePh)_2$" units (Scheme 2). In agreement with this, small amounts of $Hg(SePh)_2$ could be crystallized upon layering supernatant reaction solutions of **3** during which the formation of HgTe was not observed. Formal occupation of the tetrahedral hole by a mercury atom would lead to an ideal tetrahedral fragment of the cubic sphalerite structure. The diameter of the cluster core taken as the distance from the Hg atom at the vertex of the tetrahedron to the center of the opposite tetrahedral face is about 1500 pm.

Whereas the known cluster $[Hg_{32}Se_{14}(SePh)_{36}]$[10,11] is, according to theoretical considerations, a larger homolog of the cluster $[Hg_{17}Se_4(SePh)_{28}]^{2-}$, compound **3** is in fact a larger homolog of the cluster $[Hg_{10}Te_4(SePh)_{12}(PPhnPr_2)_4]$.[14] In contrast to the predicted formula by Dance et al. for such a group 12−16 metal chalcogenide cluster $[M_{35}E_{28}(ER)_{24}(PR_3)_4]^{10-}$ (M = Zn, Cd, Hg; E = S, Se, Te) we observed in **3**, a formal exchange of E^{2-} ions by additional ER^- ligands resulting in an overall zero charge. These 12 additional $SePh^-$ ligands are therefore each bridging three mercury atoms in contrast to the other 24 μ_2-$SePh^-$ ligands, a bonding mode which had not been observed before for $SePh^-$ ligands in group 12−16 cluster molecules. Although all mercury atoms Hg1−Hg34 have distorted tetrahedral coordination geometries, three different atomic environments coexist. The atoms Hg1−Hg4 are each coordinated by one phosphorous atom (P1−P4) of the PPh*n*Pr$_2$ ligands and three selenium atoms of the μ_2-$SePh^-$ ligands (Se13−Se24) (for selected bond length and angles see Table 1). Six of the mercury atoms namely Hg5−Hg10 are each bonded to four selenium atoms, two of them belonging to the remaining μ_2-$SePh^-$ ligands (Se25−Se36) and two of them to the μ_3-$SePh^-$ ligands (Se1−Se12). The remaining 24 mercury atoms (Hg11−Hg34) are each surrounded by two selenium atoms from either the two μ_2-$SePh^-$ ligands or the two μ_3-$SePh^-$ ligands and two tellurium atoms from the μ_3-Te^{2-} ligands (Te1−Te16). The Hg−SePh bond lengths and the Hg−Te bond lengths which range from 262.1−293.3(4) pm and 268.4−279.3(3) pm respectively correspond to those found in **1** but show a broader range due to larger distortions of the ideal tetrahedral cluster molecule.

Interestingly a similar cluster core structure was predicted by Spanhel et al. for a group 12−16 cluster of the formal composition $[Cd_{34}Se_{19}(COOCH_3)_{25}(OH)(P\mathit{n}Bu_3)_{7.5}]$ on the basis of a powder X-ray pattern, SAXS, chemical elemental analysis and FTIR spectroscopy.[15] They derived this structure from similar cage like tetrahedral pyramids (Koch pyramids) which are well known from fractal geometry.[16] According to this, the cluster structure "$Hg_{34}Te_{16}(SePh)_{36}$" corresponds to the third hierarchical level of self-similar Koch pyramids with a fractal dimension 2.

UV/Vis Spectroscopy

To investigate the electronic structure of the cluster-molecules, we measured the UV/Vis reflectance spectra of **1**−**3** as nujol mulls. The spectra are shown in Figure 4. A systematic behavior is seen for the absorption onsets reflecting the position of the first optically allowed transition. The onset shows a small shift to lower energy upon substitution of the atom in the E′ position from Se to Te in

Table 1. Selected mean interatomic distances [pm] and angles [deg] for $[Hg_{34}Te_{16}(SePh)_{36}(PPhnPr_2)_4]$ (**3**)

Coordination environment	Atoms	Range of distances [pm]	Range of angles [deg]
PHg$(SePh)_3$	Hg1−Hg4	Hg2−P2: **254.4(10)** − Hg4−P4: **255.7(11)**	P2−Hg2−Se18: **101.6(3)** − P2−Hg2−Se16: **117.5(2)**
		Hg2−Se16: **263.0(3)** − Hg2−Se18: **268.7(4)**	Se17−Hg2−Se18: **96.8(1)** − Se16−Hg2−Se17: **116.8(1)**
Hg$(SePh)_4$	Hg5−Hg10	Hg5−Se25: **262.1(3)** − Hg8−Se8: **275.1(4)**	Se7−Hg8−Se8: **97.8(1)** − Se33−Hg9−Se9: **118.5(1)**
$(Te)_2$**Hg**$(SePh)_2$	Hg11−Hg34	Hg27−Se21: **273.1(4)** − Hg14−Se4: **293.3(4)**	Te10−Hg17−Te11: **132.2(1)** − Te15−Hg20−Te13: **140.2(9)**
		Hg16−Te4: **268.4(2)** − Hg34−Te8: **279.2(3)**	Se17−Hg29−Te16: **91.6(1)** − Te7−Hg34−Se34: **115.1(1)**
			Se18−Hg32−Se33: **97.5(2)** − Se16−Hg21−Se28: **105.1(1)**
μ_3-**Te**$(Hg)_3$	Te1, Te5, Te9, Te13	Hg16−Te1: **271.4(3)** − Hg22−Te13: **273.8(3)**	Hg30−Te13−Hg20: **90.6(1)** − Hg23−Te5−Hg24: **95.1(1)**
	Te2−Te4, Te6−Te8	Hg16−Te4: **268.4(2)** − Hg34−Te8: **279.2(3)**	Hg24−Te7−Hg25: **89.9(1)** − Hg32−Te16−Hg29: **98.1(1)**
	Te10−Te12, Te14−Te16		
μ_3-**Se**$Ph(Hg)_3$	Se1−Se12	Hg10−Se11: **266.0(4)** − Hg14−Se4: **293.3(4)**	Hg6−Se3−Hg22: **103.8(1)** − Hg18−Se7−Hg20: **123.4(1)**
μ_2-**Se**$Ph(Hg)_2$	Se13−Se24	Hg2−Se16: **262.9(3)** − Hg25−Se23: **279.6(4)**	Hg3−Se21−Hg27: **100.7(1)** − Hg2−Se17−Hg29: **110.1(1)**
	Se25−Se36	Hg5−Se25: **262.1(3)** − Hg13−Se30: **283.2(4)**	Hg9−Se33−Hg32: **106.5(1)** − Hg7−Se30−Hg13: **111.3(1)**

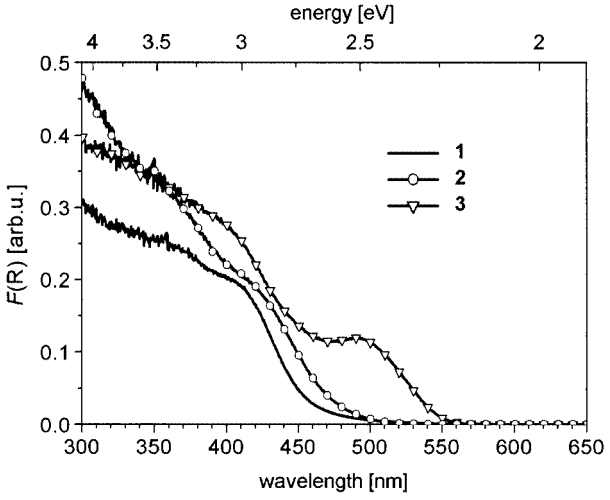

Figure 4. Reflectance spectra of $[Hg_{10}Te_4(SePh)_{12}(PPhnPr_2)_4]$ (**1**), $[Hg_{10}Te_4(TePh)_{12}(PPhnPr_2)_4]$ (**2**) and $[Hg_{34}Te_{16}(SePh)_{36}(PPhnPr_2)_4]$ (**3**) as microcrystalline powders in oil between two quartz plates.

$[Hg_{10}Te_4(E'Ph)_{12}(PPhnPr_2)_4]$ (**1**, **2**). This is consistent with the known dependence of the band gap in the corresponding bulk semiconductors HgTe and HgSe. An increase of cluster size in **3** is accompanied by a shift of the band gap to lower energies of about 0.5 eV compared with **1**. This can be interpreted in terms of the quantum confinement effect observed in larger group 12−16 nanocrystals. For **1** and **2** the spectra display two weakly resolved absorption shoulders at 400/355 nm and 410/355 nm respectively, a pattern which was also observed for $[Hg_{10}Se_4(SePh)_{12}(PPh_2nPr)_4]$ and $[Cd_{10}E_4(E'Ph)_{12}(PR_3)_4]$ (E = Se, Te; E′ = S, Se, Te).[10,17] Cluster **3** shows one well resolved absorption maximum at 493 nm followed by a further broad shoulder extending to 300 nm which shows no distinct maximum. The spectrum of **3** is therefore different from those of $[Cd_{32}Se_{14}(SePh)_{36}(PPh_3)_4]$ and $[Hg_{32}Se_{14}(SePh)_{36}]$ which both show two distinct absorption maxima in the low energy region of the spectra.[1,10] Furthermore the first electronic transition for $[Hg_{32}Se_{14}(SePh)_{36}]$ lies 50 nm lower in energy at 550 nm compared with **3** although the latter contains two additional mercury atoms and 16 tellurium atoms instead of the selenium atoms. These absorption features are therefore most probably related to the difference in the structure of the cluster core in particular the mercury vacancy in the center of **3**. The dissolution of **3** in THF at −25 °C followed by careful warming to room temperature resulted in a clear orange solution which showed an absorption spectrum similar to that of the crystalline powder as a mull in oil. This is also evidence for the stability of **3** in solution at room temperature.

Compound **2** dissolved in THF at −25 °C to yield a clear red orange solution from which a deep red microcrystalline powder precipitated upon warming to room temperature. The X-ray powder diffraction pattern shows in the low 2 theta region (2θ = 2−7 deg.) several well resolved peaks suggesting crystallization of cluster molecules. Furthermore, this red powder displays an absorption onset at 650 nm with a shoulder at about 530 nm. The elemental analysis (found C 18.69, H 1.46%) shows unusually good agreement with the calculated values for the formula $[Hg_{34}Te_{16}(TePh)_{36}](PPhnPr_2)_4]$ (calcd. C 18.64, H 1.52%).

Theory

Density functional investigations have been carried out to elucidate certain features of **3**. All calculations were performed with the RI-DFT modules[18] (RI means the "resolution of the identity", i.e. an auxiliary basis set expansion is used, to process Coulomb-energy contributions more efficiently) of the TURBOMOLE[19] program system employing the BP86-functional,[20] which is a rather reliable functional for treatment of transition metal compounds, and (if not mentioned otherwise) a "split valence plus polarization" basis set − SV(P)[21] − where the brackets indicate that the polarization functions were omitted for H.

The first point of interest concerns the hole in the center of **3**. A condensation of **1** might also be expected to lead to a "real cubic sphalerite cluster" with one further mercury atom in the vacancy (and perhaps two phosphane ligands being replaced by μ_1-$SePh^-$ to maintain the overall zero charge). Thus we performed geometry optimizations of the model clusters $[Hg_{34}Te_{16}(SeMe)_{36}(PMe_3)_4]$, $[Hg_{35}Te_{16}(SeMe)_{36}(PMe_3)_4]^{2+}$ (both *T*-symmetry) and $[Hg_{35}Te_{16}(Se-$

$Me)_{38}(PMe_3)_2]$ (*C*2-symmetry). A drastic lowering of the HOMO−LUMO gap was observed upon introducing μ_1-SeR^- ligands (from 1.52 eV for $[Hg_{34}Te_{16}(SeMe)_{36}(PMe_3)_4]$ and 1.17 eV in $[Hg_{35}Te_{16}(SeMe)_{36}(PMe_3)_4]^{2+}$ to only 0.23 eV for $[Hg_{35}Te_{16}(SeMe)_{38}(PMe_3)_2]$), which indicates that this kind of coordination should be unfavorable. Another way of obtaining a neutral cluster with 35 Hg atoms might be substitution of two μ_3-SeR^- ligands by Te^{2-}, but in the observed condensation reaction all Te^{2-} available from **1** is already incorporated in the structure with the central hole, so if there is no other source of chalcogenide dianions, the loss of electroneutrality might be one reason for the formation of **3**. However, geometrical reasons also seem at a first glance to prevent a "filled" cluster core because the vacancy is simply not large enough to be occupied by Hg^{2+}. The computed Te−Te distances of 398.7 pm for $[Hg_{34}Te_{16}(SeMe)_{36}(PMe_3)_4]$ in the central Te_4-unit would lead to Hg−Te distances of 244.1 pm for a mercury atom in the center of this Te_4-tetrahedron while the Te−Te distances found in the X-ray structure of **3** are even shorter (376.4−385.5 pm). It seems as if the $PhSe^-$-ligands on the edges of this mixed chalcogenide cluster are responsible for this, because the predicted value for a hypothetical $[Hg_{34}Te_{16}(TeMe)_{36}(PMe_3)_4]$ cluster is 434.2 pm which is only slightly shorter than the observed Te−Te distance (456 pm) and the Hg−Te bond length (279 pm) in bulk HgTe.[13] The insertion of a central Hg^{2+} in **3**, leading to $[Hg_{35}Te_{16}(SeMe)_{36}(PMe_3)_4]^{2+}$, resulted in a significant increase of the predicted Te−Te distances with values of 470.7 pm which might cause high tension and reduced stability for the latter system. Interestingly however, the size of the tetrahedron of the outer Hg-atoms (Hg1−Hg4 in Figure 3) only increased from 1722.5 pm to 1754.7 pm when going from $[Hg_{34}Te_{16}(SeMe)_{36}(PMe_3)_4]$ to $[Hg_{35}Te_{16}(SeMe)_{36}(PMe_3)_4]^{2+}$ and all other bond lengths did not change by more than 7 pm. The tension caused by the stretching of the central Te_4 tetrahedra is rather compensated for by a deformation of the bond angles which is of course mostly significant for the four tellurium atoms in the center (Te1, Te5, Te9, Te13) changing from μ_3-bridging (Hg−Te−Hg: 92.86°) to a distorted tetrahedral coordination (Hg−Te−Hg: 104.73−113.87°) while all the other bond angles did not change by more than 4.3°. These findings suggest that from the theoretical point of view such an ionic cluster molecule could be stable but its formation is not favored in the present reaction due to the absence of an appropriate counterion.

$[Hg_{32}Se_{14}(SePh)_{36}]$ and **3** are obviously different in their coordination behavior towards phosphane ligands. Although both clusters are synthesized starting from phosphane-coordinated "Hg_{10}" cluster molecules, **3** appears with all four Hg corners saturated by $PPhnPr_2$ whereas in the cluster with 32 mercury atoms all four mercury atoms at the corners are only trigonally coordinated by three $SePh^-$ ligands. Since a comparison of the influence of the phosphane ligands on the electronic structure of $[Hg_{34}Te_{16}(SeMe)_{36}(PMe_3)_4]$ and $[Hg_{32}Se_{14}(SeMe)_{36}(PMe_3)_4]$ showed no real differences between these two model compounds, we performed further geometry optimizations of the more realistic systems $[Hg_{34}Te_{16}(SePh)_{36}(PMe_3)_4]$, $[Hg_{34}Te_{16}(SePh)_{36}(PPh_3)_4]$, $[Hg_{32}Se_{14}(SePh)_{36}(PMe_3)_4]$, and $[Hg_{32}Se_{14}(SePh)_{36}(PPh_3)_4]$. This however was only possible using two different small basis sets (single zeta quality) for the organic ligands, which are specially optimized for the description of phenyl- and methyl-substituents (available as "SZ.benzene" and "sz.methane" in TURBOMOLE). The energies for the detachment of the PMe_3 ligands from $[Hg_{34}Te_{16}(SePh)_{36}(PMe_3)_4]$ and $[Hg_{32}Se_{14}(SePh)_{36}(PMe_3)_4]$ are quite similar (+44.6 kJ/mol and +43.8 kJ/mol per ligand, respectively). In contrast to this, the corresponding Hg−P bond strengths are clearly lower in the case of PPh_3 (+23.2 kJ/mol in $[Hg_{34}Te_{16}(SePh)_{36}(PPh_3)_4]$ and only +7.8 kJ/mol in $[Hg_{32}Se_{14}(SePh)_{36}(PPh_3)_4]$), which can be explained by the higher steric demands of the phenyl substituent. Especially in the $[Hg_{32}Se_{14}(SePh)_{36}]$ cluster core the μ_2-$SePh^-$ groups near the terminal Hg-atoms protrude so much that repulsion effects prevent a stronger metal-ligand interaction. The nuclear arrangement in the clusters with 34 Hg-atoms, i.e. in a $[Hg_{34}Te_{16}(SePh)_{36}]$ cluster core, is more favorable for the uptake of bulky ligands, and additionally, the experiments leading to **3** were carried out with $PPhnPr_2$. The steric properties of the latter phosphane should be somewhere in between those of PMe_3 and PPh_3. This clearly accounts for the experimental findings.

The differences between the UV/Vis spectra of **3** and $[Hg_{32}Se_{14}(SePh)_{36}]$ are also in line with theoretical results obtained by time dependent DFT as shown in Table 2. Electronic excitations were calculated using the TURBOMOLE module "ESCF".[22,23] The experimental absorbance maximum of **3** appears at 493 nm, which means an excitation energy of 2.51 eV, whereas two distinct maxima in $[Hg_{32}Se_{14}(SePh)_{36}]$ are located at 2.27 eV and 2.47 eV. Once again, for the model compounds $[Hg_{34}Te_{16}(SeMe)_{36}(PMe_3)_4]$ and $[Hg_{32}Se_{14}(SeMe)_{36}]$, we calculated the energies of the twenty lowest singlet transitions in the dipole-allowed irreducible representation *t*. The red-shift of time dependent DFT[24] was taken into account by adding a systematic offset of 0.8 eV. As a result, there are two strong low energy

Table 2. Comparison of experimental and calculated (TDDFT) spectra of $[Hg_{32}Se_{14}(SePh)_{36}]$ and $[Hg_{34}Te_{16}(SeMe)_{36}(PMe_3)_4]$.

	Transition energy (exp.) in eV	Transition energy (TDDFT) in eV	Oscillator strength (TDDFT)
$Hg_{32}Se_{14}(SePh)_{36}$	2.27	2.221	0.30
	2.47	2.353	0.05
$Hg_{34}Te_{16}(SeMe)_{36}(PMe_3)_4$	2.51	2.411	0.25
		2.495	0.10

transitions in the predicted spectrum of $[Hg_{34}Te_{16}(SeMe)_{36}(PMe_3)_4]$ at 2.41 eV and 2.49 eV − the experimental procedure might not be able to resolve this small energetic separation which would explain the solitary maximum at 2.51 eV in the spectrum of **3**. For $[Hg_{32}Se_{14}(SeMe)_{36}]$, apart from transitions with negligibly small oscillator strengths, one also finds two important excitations at 2.22 eV and 2.35 eV, which closely resemble the measured values in the spectrum of the corresponding phenyl cluster (it should be noted, that the calculated oscillator strength of the second transition is smaller than for the first excitation, which is also the case in the experimental spectrum, though however not to this extent).

Conclusions

We have shown that reactions of $HgCl_2$ with $PPhnPr_2$, $Te(SinBu_3)_2$ and $PhESiMe_3$ (E = Se, Te) in DME result in the formation of $[Hg_{10}Te_4(EPh)_{12}(PPhnPr_2)_4]$ (E = Se **1,** E = Te **2**). Investigations in solution reveal that the cluster $[Hg_{10}Te_4(SePh)_{12}(PPh_2nPr)_4]$ (**1**) is a metastable compound which is converted in benzene/toluene at room temperature to $[Hg_{34}Te_{16}(SePh)_{36}(PPhnPr_2)_4]$ (**3**). The "$Hg_{34}Te_{16}Se_{36}$" cluster core of **3** consists of four tetrahedral "$Hg_{10}Te_4(SePh)_{12}$" cages each sharing three "$Hg(SePh)_3$" edges, a cage structure well known in fractal geometry as a "Koch pyramid". Thus the structure can be described as an ideal tetrahedral fragment, 1500 pm in diameter, of the cubic sphalerite lattice with one mercury vacancy in the center. The molecular structure of **3** with mixed chalcogen atoms is therefore different from that of $[Hg_{32}Se_{14}(SePh)_{36}]$ which is a product of the recrystallization of the pure selenide cluster $[Hg_{10}Se_4(SePh)_{12}(PPh_2nPr)_4]$.[10] DFT calculations reveal that an ionic cluster $[Hg_{35}Te_{16}(SeMe)_{36}(PMe_3)_4]^{2+}$ in which the vacancy is filled by a mercury ion could also be stable. This suggests that the formation of the vacancy is probably mostly driven by the absence of an appropriate counterion in the reaction which would stabilize such an ionic cluster molecule. This peculiarity of the structure has also a distinct influence on the electronic structure of **3** in comparison with $[Hg_{32}Se_{14}(SePh)_{36}]$ as can be seen from the UV/Vis reflectance spectra. In future we will target the development of conditions for further controlled cluster growth of these molecules.

Experimental Section

Standard Schlenk techniques were employed throughout the syntheses using a double manifold vacuum line with high purity dry nitrogen. The solvents tetrahydrofuran (THF), dimethylethylene glycol (DME) and benzene were dried over sodium-benzophenone and toluene over $LiAlH_4$, and distilled under nitrogen. Anhydrous $HgCl_2$ was purchased from Aldrich. $PhSeSiMe_3$,[24] $Se(SiMe_3)_2$ [25] and $PhTeSiMe_3$ [26] were prepared according to standard literature procedures. $Te(SinBu_3)_2$ was prepared accordingly to the synthesis of $Se(SiMe_3)_2$ by the use of $ClSinBu_3$ instead of $ClSiMe_3$.

UV/Vis absorption spectra of cluster molecules in solution were measured on a Varian Cary 500 spectrophotometer in quartz corvettes. Solid state reflection spectra were measured as micron sized crystalline powders between quartz plates with a Labsphere integrating sphere.

1: $HgCl_2$ (0.27 g, 0.99 mmol) was dissolved in DME (40 mL) with the addition of $PPhnPr_2$ (0.42 mL, 1.99 mmol). $PhSeSiMe_3$ (0.34 mL, 1.79 mmol) was then added at 0 °C and the resultant clear yellow solution stirred for half an hour. Addition of $Te(SinBu_3)_2$ (0.14 mL, 0.3 mmol) at −40 °C led to the formation of a pale yellow solution from which $[Hg_{10}Se_4(TePh)_{12}(PPhnPr_2)_4]$ (**1**) could be crystallized at −30 °C (60% yield). $C_{120}H_{136}Hg_{10}P_4Se_{12}Te_4$ (5166.11): calcd. C 27.89, H 2.65; found C 27.79, H 2.72.

2: $HgCl_2$ (0.23 g, 0.85 mmol) was dissolved in DME (35 mL) with the addition of $PPhnPr_2$ (0.36 mL, 1.69 mmol). $PhTeSiMe_3$ (0.31 mL, 1.36 mmol) was then added at 0 °C and the resultant clear yellow solution stirred for an hour. Addition of $Te(SinBu_3)_2$ (0.12 mL, 0.25 mmol) at −40 °C led to the formation of a pale yellow solution from which $[Hg_{10}Te_4(TePh)_{12}(PPhnPr_2)_4]$ (**2**) could be crystallized at −30 °C (63% yield). $C_{120}H_{136}Hg_{10}P_4Te_{16}$ (5749.79): calcd. C 25.06, H 2.38; found C 24.95, H 2.26.

3: Compound **1** (0.11 g, 0.019 mmol) was dissolved in a mixture of benzene (4 mL) and toluene (16 mL) at 5 °C giving an orange solution. The solution was then gradually allowed to warm up in the cooling bath and over the period of one week orange crystals of $[Hg_{34}Te_{16}(SePh)_{36}(PPhnPr_2)_4]$ (**3**) were formed (yield 70% calculated for Scheme 2). $C_{264}H_{256}Hg_{34}P_4Se_{36}Te_{16}$ (15257.05): calcd. C 20.78, H 1.69; found C 20.41, H 1.60.

Crystals suitable for single-crystal X-ray diffraction were obtained directly from the reaction solutions of the compounds and then selected in perfluoroalkyl ether oil.

Single-crystal X-ray diffraction data were collected using graphite-monochromated Mo-K_α radiation (λ = 0.71073 Å) on a STOE IPDS II (Imaging Plate Diffraction System). The structures were solved with the direct methods program SHELXS[27] of the SHELXTL PC suite of programs and were refined with the use of the full-matrix least-squares program SHELXL.[28] Molecular diagrams were prepared using the program SCHAKAL 97[28] and DIAMOND.[29]

All Hg, Te, Se and P atoms were refined with anisotropic displacement parameters. In **2** the C atoms were also refined anisotropically. The C atoms in **1** were refined isotropically while the C atoms of the phenyl groups in **3** were refined isotropically as rigid groups. H atoms of the SePh groups were included in calculated positions for **2**. C_6H_6 solvent molecules in **3** were refined as rigid groups with half occupancy. Residual electron density in the difference Fourier map of **3** indicates the existence of additional disordered solvent molecules in the crystal lattice which could not be refined successfully (see Table 3).

Numerical absorption corrections were applied to the data of **2** and **3**.

CCDC-205710 (**1**), -205711 (**2**), and -205712 (**3**) contain the supplementary crystallographic data for this paper. These data can be obtained free of charge at www.ccdc.cam.ac.uk/conts/retrieving.html (or from the Cambridge Crystallographic Data Centre, 12 Union Road, Cambridge CB2 1EZ, UK; Fax: (internat.) + 44-1223-336-033; E-mail: deposit@ccdc.cam.ac.uk).

Table 3. Crystallographic data for $[Hg_{10}Te_4(SePh)_{12}(PPhnPr_2)_4]$ (**1**), $[Hg_{10}Te_4(TePh)_{12}(PPhnPr_2)_4]$ (**2**) and $[Hg_{34}Te_{16}(SePh)_{36}(PPhnPr_2)_4]$ (**3**)

	1	**2**	**3**·2C$_6$H$_6$
Formula mass	5165.99	5749.67	15413.0
Crystal system	tetragonal	tetragonal	triclinic
Space group	$I4_1/a$	$I4_1/a$	$P\bar{1}$
a [pm]	2550.7(4)	2601.9(4)	2468.4(5)
b [pm]			3109.8(6)
c [pm]	2164.2(4)	2187.1(4)	3163.9(6)
α [°]			104.41(3)
β [°]			108.35(3)
γ [°]			103.31(3)
V [10^{6}pm^3]	14081(4)	14807(4)	21031(7)
Z	4	4	2
T [K]	180	180	210
d_c [g cm^{-3}]	2.437	2.579	2.434
μ(Mo-K_α) [mm^{-1}]	14.859	13.499	16.607
F[000]	9328	10192	13520
$2\theta_{max}$ [°]	52	52	44.5
Measured reflections	31108	18281	98038
Unique reflections	6892	6694	49871
R_{int}	0.0966	0.1103	0.0958
Reflections with $I > 2\sigma(I)$.	5111	4744	20920
Refined parameters	213	339	1463
$R1[I > 2\sigma(I)]$[a]	0.0404	0.0468	0.0581
$wR2$(all data)[b]	0.1308	0.1441	0.1974

[a] $R1 = \Sigma||F_o| - |F_c||/\Sigma|F_o|$. [b] $wR2 = \{\Sigma[w(F_o^2 - F_c^2)^2]/\Sigma[w(F_o^2)^2]\}^{1/2}$.

X-ray powder diffraction patterns (XRD) were measured on a STOE STADI P diffractometer (Cu-K_α radiation, Germanium monochromator, Debye−Scherrer geometry) in sealed glass capillaries. Theoretical powder diffraction patterns for **1** and **2** were calculated on the basis of the atom coordinates obtained from single-crystal X-ray analysis by using the program package STOE WinXPOW.[30]

Acknowledgments

This work was supported by the Deutsch-Israelisches Programm (DIP) and the Deutsche Forschungsgemeinschaft (Center for Functional Nanostructures CFN). A. E. is grateful to Prof. D. Fenske for helpful discussions and for providing excellent working conditions, E. Tröster for her invaluable assistance in the practical work and Dr. Susan Anson for careful revision of the manuscript.

[1] V. Soloviev, A. Eichhöfer, D. Fenske, U. Banin, *J. Am. Chem. Soc.* **2001**, *123*, 2354−2364.
[2] A. Eichhöfer, O. Hampe, M. Blom, *Eur. J. Inorg. Chem.* **2003**, 1307 −1314; S. Behrens, M. Bettenhausen, A. Eichhöfer, D. Fenske, *Angew. Chem.* **1997**, *109*, 2874−2876; *Angew. Chem. Int. Ed. Engl.* **1997**, *24*, 2797−2799; S. Behrens, D. Fenske, *Ber. Bunsenges. Phys. Chem.* **1997**, *101*, 1588−1592.
[3] B. Ali, I. G. Dance, D. C. Craig, M. L. Scudder, *J. Chem. Soc., Dalton Trans.* **1998**, 1661−1667; M. D. Nyman, M. J. Hampden-Smith, E. N. Duesler, *Inorg. Chem.* **1996**, *35*, 802−803.
[4] A. Eichhöfer, D. Fenske, H. Pfistner, M. Wunder, *Z. Anorg. Allg. Chem.* **1998**, *624*, 1909−1914.
[5] H. Pfistner, D. Fenske, *Z. Anorg. Allg. Chem.* **2001**, *627*, 575−582.
[6] G. S. H. Lee, K. J. Fisher, D. C. Craig, M. L. Scudder, I. G. Dance, *J. Am. Chem. Soc.* **1990**, *112*, 6435−6437; G. S. H. Lee, D. C. Craig, I. Ma, M. L. Scudder, T. D. Bailey, I. G. Dance, *J. Am. Chem. Soc.* **1988**, *110*, 4863−4864; I. G. Dance, A. Choy, M. L. Scudder, *J. Am. Chem. Soc.* **1984**, *106*, 6285−6295.
[7] T. Vossmeyer, G. Reck, L. Katsikas, E. T. K. Haupt, B. Schulz, H. Weller, *Science* **1995**, *267*, 1476−1479; T. Vossmeyer, G. Reck, B. Schulz, L. Katsikas, H. Weller, *J. Am. Chem. Soc.* **1995**, *117*, 12881−12882.
[8] A. Rogach, S. Kershaw, M. Burt, M. Harrison, A. Kornowski, A. Eychmüller, H. Weller, *Adv. Mater.* **1999**, *11*, 552−555.
[9] M. Harrison, S. Kershaw, A. Rogach, A. Kornowski, A. Eychmüller, H. Weller, *Adv. Mater.* **2000**, *12*, 123−125.
[10] A. Eichhöfer, E. Tröster, *Eur. J. Inorg. Chem.* **2002**, 2253−2256.
[11] S. Behrens, M. Bettenhausen, A. C. Deveson, A. Eichhöfer, D. Fenske, A. Lohde, U. Woggon, *Angew. Chem.* **1996**, *108*, 2360−2363; *Angew. Chem. Int. Ed. Engl.* **1996**, *35*, 2215−2218.
[12] Landolt-Börnstein, *Gruppe III: Kristall und Festkörperphysik*, vol. 17, *Halbleiter* (Ed.: O. Madelung), Springer, Berlin, **1982**, p. 236.
[13] J. Waser, L. Pauling, *J. Chem. Phys.* **1950**, *18*, 747.
[14] E. Schulz Lang, R. A. Zan, C. C. Gatto, R. A. Burrow, E. M. Vázquez-López, *Eur. J. Inorg. Chem.* **2002**, 331−333.
[15] I. Dance and G. Lee in *Perspectives in Coordination Chemistry* (Ed.: A. F. Williams) Helvetica Chimica Acta Basel; VCH, Weinheim, **1992**, p. 86−94.
[16] V. Ptatschek, T. Schmidt, M. Lerch, G. Müller, L. Spanhel, A. Emmerling, J. Fricke, A. H. Foitzik, E. Langer, *Ber. Bunsenges. Phys. Chem.* **1998**, *102*, 85−95.
[17] H. O. Peitgen, H. Jürgens and D. Saupe in *Bausteine des Chaos − Fraktale*, Springer Berlin, Klett-Cotta, Stuttgart, **1992**.
[18] A. Eichhöfer, A. Aharoni, U. Banin, *Z. Anorg. Allg. Chem.* **2002**, *628*, 2415−2421.
[19] O. Treutler, R. Ahlrichs, *J. Chem. Phys.* **1995**, *102*, 346; K. Eichkorn, O. Treutler, H. Öhm, M. Häser, R. Ahlrichs, *Chem. Phys. Lett.* **1995**, *242*, 652, K. Eichkorn, F. Weigend, O. Treutler, R. Ahlrichs, *Theo. Chem. Acc.* **1997**, *97*, 119.
[20] M. Bär, M. Häser, H. Horn, C. Kölmel, R. Ahlrichs, *Chem. Phys. Lett.* **1989**, *162*, 165.
[21] A. D. Becke, *Phys. Rev. A* **1988**, *38*, 3098; S. H. Vosko, L. Wilk, M. Nusair, *Can. J. Phys.* **1980**, *58*, 1200; J. P. Perdew, *Phys. Rev. B* **1986**, *33*, 8822.
[22] A. Schäfer, H. Horn, R. Ahlrichs, *J. Chem. Phys.* **1992**, *97*, 2571.
[23] R. Bauernschmitt, R. Ahlrichs, *Chem. Phys. Lett.* **1996**, *256*, 454.
[24] R. Bauernschmitt, R. Ahlrichs, *J. Chem. Phys.* **1996**, *104*, 9047.
[25] N. Miyoshi, H. Ishii, K. Kondo, S. Mui, N. Sonoda, *Synthesis* **1979**, 301−304.
[26] H. Schmidt, H. Ruf, *Z. Anorg. Allg. Chem.* **1963**, *321*, 270−273.
[27] K. Praefcke, C. Weichsel, *Synthesis* **1980**, 216.
[28] G. M. Sheldrick, SHELXTL PC version 5.1 An Integrated System for Solving, Refining, and Displaying Crystal Structures from Diffraction Data, Bruker Analytical X-ray Systems, Karlsruhe, **2000**.
[29] E. Keller, SCHAKAL 97, A Computer Program for the Graphic Representation of Molecular and Crystallographic Models, Universität Freiburg, **1997**.
[30] K. Brandenburg, DIAMOND version 2.1d, Visual Crystal Structure Information System, Bonn, **2000**.
[31] STOE, WinXPOW, STOE & Cie GmbH, Darmstadt, **2000**.

Received July 9, 2003
Early View Article
Published Online November 19, 2003

